



Effects of Multi-Charge on Aerosol Hygroscopicity Measurement by HTDMA

Chuanyang Shen¹, Gang Zhao^{1,2}, Chunsheng Zhao¹

¹Department of Atmospheric and Oceanic Sciences, School of Physics, Peking University, Beijing 100871, China

5 ²College of Environmental Sciences and Engineering, Peking University, Beijing 100871, China

Correspondence to: Chunsheng Zhao (zcs@pku.edu.cn)

Abstract. The Humidified Tandem Differential Mobility Analyzer (HTDMA) is widely used to obtain the hygroscopic properties of submicron particles. Aerosol size-resolved hygroscopicity parameter κ measured by HTDMA will be influenced by the contribution of multiply charged aerosols, and this effect has seldom been discussed in previous field measurements. Our calculation demonstrates that the number ratio of multiply charged particles is quite considerable for some specific sizes between 100 nm and 300 nm, especially during the polluted episode. The multi charges will further lead to the weakening effect of aerosol hygroscopicity in HTDMA measurements. Therefore, we propose a new algorithm to do the multi-charge correction for the size-resolved hygroscopicity κ considering both the weakening effect and multi-charge number contribution. The application in field measurements shows that the relatively high hygroscopicity in accumulation size range will lead to the overestimation of the particle's hygroscopicity smaller than 200 nm. The low hygroscopicity in coarse mode particles will lead to the underestimation of accumulation particles between 200 nm and 500 nm. The difference between corrected and measured κ can reach as large as 0.05, highlighting that special attention needs to be paid to the multi-charge effect when the HTDMA is used for the aerosol hygroscopicity measurement.

1 Introduction

20 Atmospheric particles can affect the Earth-Atmosphere system through the interaction with solar radiation, and acting as cloud nuclei (ALBRECHT, 1989; CHARLSON et al., 1992; Guo et al., 2017; Haywood & Boucher, 2000; Lohmann & Feichter, 2005 2001; Penner, Hegg, & Leaitch, 2001; Twomey, 1974). They can also impact human life by degrading visibility and despairing respiratory health (Chang, Song, & Liu, 2009; Ibald-Mulli, Wichmann, Kreyling, & Peters, 2002; Su et al., 2017). All these effects are closely related to aerosol's hygroscopic property (Kreidenweis & Asa-Awuku, 2014), which reflects the aerosol's ability to absorb water under a specific relative humidity (RH).

Nowadays, there are many instruments that have been used to characterize aerosol particle's hygroscopicity, and HTDMA is one of the most widely used. As it can directly give the particle's size distribution after water uptake, it can be employed to obtain both the mixing state and bulk mean hygroscopic properties of ambient aerosol particles (Swietlicki et al., 2017). Two Differential Mobility Analyzers (Swietlicki et al.) are used in this technique to quantify the size change of particles under different RH exposure. The measured distribution function (MDF) is skewed and smoothed from the particle's actual growth factor probability density function (GF-PDF). So several inversion algorithms have been developed to inverse the true GF-



PDF (Cubison, Coe, & Gysel, 2005; Gysel, McFiggans, & Coe, 2009; Stolzenburg & McMurry, 2008; Voutilainen, Stratmann, & Kaipio, 2000). These inversions include the TDMAfit algorithm, the optimal estimation method (OEM) and TDMAinv algorithm. However, these algorithms are based on the assumption that the particles sampled are dominated by singly charged particles. Under this condition, the forward function can be simplified and data analysis is limited within the size concerned, not interfered by other sizes. If the number fraction of multiply charged particles at the selected dry diameter becomes significant, the measured results will be affected by the contributions from other dry sizes. In this case, appropriate data inversion is quite complicated.

However, in some special cases, the accurate data inversion for multi-charge particles can be achieved when the sampled particles are exclusively doubly or triply charged. Duplissy et al. (2008) obtained the kernel functions for multiply charged particles and applied them in the data inversion to retrieve the correct GFs. The dry sizes he selected are dominated by doubly or triply charged particles. However, in most field measurements, this assumption is invalid. As far as we are concerned, no previous studies have done the multi-charge correction for atmospheric aerosol particles in the HTDMA measurement. The effect of multi-charge correction on the size-resolved hygroscopicity is also not fully evaluated for atmospheric aerosols.

In this study, we first analyse the number contribution from particles carrying different charges. Then we present the weakening effect of multiply charged particle's hygroscopicity in the HTDMA measurement. These two effects were included into the algorithm to do the multi-charge correction for particle's size-resolved hygroscopicity. Then the application and corresponding influences of multi-charge correction on particle's hygroscopicity were discussed.

2 Multi-Charge Effects

2.1 Number Contribution from multiply charged particles

In the sizing process of the DMA, only particles within a narrow range of electrical mobility (Z_p) can transmit through the classifier exit slit and come to the downstream humidification and size distribution measurement system. The electrical mobility is defined as:

$$Z_p = \frac{neC(D_p)}{3\pi\mu D_p} \quad (1)$$

where $C(D_p)$ is the Cunningham slip correction; the e is elementary charge; the n is the number of elementary charges on the particle; the μ is the gas viscosity poise and D_p is the particle's physical diameter. From the equation above, we can see that with the same electrical mobility, particles can have different combination of diameters and number of charges, and this is where multi-charge effects come from.

The range that can pass through the DMA is defined as the mobility bandwidth, ΔZ_p :



$$\Delta Z_p = \frac{q_a}{q_{sh}} Z_p^* \quad (2)$$

where the Z_p^* is the set mobility, and the q_a and q_{sh} is the aerosol flow rate and sheath air flow rate, respectively. This equation doesn't account for diffusion broadening.

We can calculate the particle charge distribution at each size based on a theoretical model developed by Wiedensohler, Lückemeier, Feldpausch, and Helsper (1986). Then the particle's probability to pass through a DMA classifier can be determined using the kernel function $G(i, x)$:

$$G(i, x) = \sum_{v=1}^{\infty} F(x, v) \Omega(x, v, i) \quad (3)$$

where the i is the diameter set in the DMA; $F(x, v)$ is the charge distribution of particles that exit from a neutralizer. $\Omega(x, v, i)$ is the probability of particles to pass through the DMA with v charges at the scale parameter x . In this study, the maximum value of v is 10.

Therefore, given a particle number size distribution (PNSD), the number of particles that can pass through the DMA with a set diameter of i is:

$$N(i) = \int_0^{\infty} G(i, x) n(x) dx \quad (4)$$

The corresponding number ratio of particles carrying different charges can also be determined.

Two aerosol size distribution cases representing the relatively clean period and polluted period during our field measurement (refer to section 4) are shown in Fig. 1. The corresponding ratio of particles carrying different charges is calculated from the PNSD using the abovementioned DMA electrical mobility and charging theory. During the polluted period when total particle volume concentration is large, an obvious feature in PNSD is that the accumulation mode larger than 100 nm grows very large. The growth of this mode leads to an increase in the proportion of multi-charged particles, especially in the size range of 100-300 nm (electrical mobility diameter). For example, when we set 100 nm in the first DMA, more than 40% of the selected particles are multiply charged. This ratio is about 30% and 20% for electrical diameter of 200 nm and 300 nm, respectively. Thus the HTDMA measured size-resolved hygroscopicity will also be influenced by those multiply charged large particles.

2.2 Weakening Effect of Hygroscopicity

In previous studies, Gysel et al. (2009) presented that the center of the kernel function at higher charges is systematically offset toward smaller GFs. An illustration figure (Fig.2) was shown to explain the cause of this effect. For electrical mobility diameter of 100 nm, the doubly and triply charged particles are about 151 nm and 196 nm, respectively. When all these three kind of particles have a true growth factor of 1.6, they will grow to the size of 160 nm, 242 nm and 314 nm. Since the number of charges they carry remain the same as before, their peak sizes in the second DMA are around 160 nm, 154 nm and 150 nm. Therefore, the growth factors they display in the HTDMA measurement is 1.6, 1.54 and 1.5, respectively. It can



be clearly seen that the growth factor is decreased or weakened. We call this phenomenon as weakening effect of growth factor or hygroscopicity brought by the multi-charge.

For each true growth factor, the HTDMA system will give a corresponding weakened growth factor, which can be calculated based on the electrical mobility theory (Fig. 2b). Each growth factor under a specific RH correspond to a hygroscopic parameter κ (Petters & Kreidenweis, 2007). Thus, the measured hygroscopicity is also weakened. As illustrated in Fig.3a, the weakening effect increases almost linearly with particle's hygroscopicity, with the slope as the weakening factor. For each electrical mobility diameter with different charges, a weakening factor of hygroscopicity can be calculated. The results are summarized in Fig.3b.

100

3 Method of Multi-Charge Correction

3.1 Multi-charge correction for size-resolved hygroscopicity

Multi-charge corrections are common when the DMA is used to scan the aerosol sizes, especially in the PNSD measurements. The shape of PNSD after multi-charge correction can be significantly different from that of the raw measured one. Therefore, it's necessary to evaluate the effect of multi-charge correction on the size-resolved hygroscopicity obtained by HTDMA. This study developed an algorithm to do the multi-charge correction for the measured values based on the work of Deng et al. (2011) and Zhao et al. (2019).

Our correction is based on the assumption that, for each electrical mobility set at DMA1, the measured mean hygroscopicity is contributed by all particles that can pass through the DMA1. All the contributing particles carry the mean hygroscopicity of its physical size. For example, when a particle with larger dry diameter (D_p^n) carrying n charges pass through the DMA1 and make a contribution to the MDF, it's hard to tell which hygroscopicity it carries because it has a probability distribution function over hygroscopicity. In our algorithm, this particle is assumed to have a hygroscopicity of the mean value in size D_p^n . This assumption is statistically right and feasible but may not be true on a single-particle scale.

When the scan diameter in the first DMA is set as D_i , the observed mean hygroscopicity K_i by HTDMA can be expressed as:

$$115 \quad K_i = \frac{1}{N(i)} \int_0^\infty G^*(i, x) K^*(x) n(x) dx \quad (5)$$

where x is the scale parameter; $K^*(x)$ is the true mean κ for the scale parameter x ; $n(x)$ is the true aerosol number size distribution; $N(i)$ is the total number concentration of particles that pass through the first DMA. The $G^*(i, x)$ is the transformed kernel function $G(i, x)$ of DMA1, which includes the weakening effect $S(i, v)$.

$$G^*(i, x) = \sum_{v=1}^\infty F(x, v) \Omega(x, v, i) S(i, v) \quad (6)$$

$$120 \quad N(i) = \int_0^\infty G(i, x) n(x) dx \quad (7)$$

So the question can be simplified as the following:



$$K_i = \int_0^\infty H(i, x) K^*(x) dx \quad (8)$$

or

$$\mathbf{K} = \mathbf{H} \mathbf{K}^* \quad (9)$$

125 where the $K^*(x)$ or \mathbf{K}^* is the true distribution of κ we want to obtain, and K_i or \mathbf{K} is the measured κ distribution. $H(i, x)$ is:

$$H(i, x) = \frac{1}{N(i)} n(x) G^*(i, x) dx \quad (10)$$

$H(i, x)$ or \mathbf{H} matrix is the forward function and can be calculated from given information. Given a true κ distribution, we should be able to calculate the measured κ distribution imposed by multi-charge effect. The \mathbf{H} matrix accounts for the DMA transfer function, the particle charge distribution, weakening factors and number distribution of particles over each size
130 parameter. The detailed steps to solve this matrix inverse problem can be found in Zhao et al. (2019).

One hypothetical κ distribution along with the corresponding multi-charge corrected κ distributions are shown in Fig.4. It represents a common case in the ambient environment: relatively low hygroscopicity for ultrafine particles, high hygroscopicity in accumulation mode size and nearly hydrophobic in the coarse mode. Two PNSD are used in the multi-charge correction, representing clean and pollution conditions. It can be seen that large variation of κ over sizes will cause
135 large difference between pre- and post-corrected κ distribution, especially when the large variation exists in the singly, doubly and triply charged particle sizes. For example, the difference between measured and corrected κ reach a peak in 150 nm and 350 nm. For electrical mobility size of 150 nm, the corresponding doubly and triply charged particles are around 235 nm and 314 nm. These three sizes are located in the area where κ increases steeply. Similarly, for electrical mobility size of 350 nm, the corresponding doubly and triply charged particles are about 605 nm and 852 nm. These three sizes are also
140 located in the area where κ drops greatly. Another point that can be seen from Fig. 4 is that an increasing trend of κ will cause the measured κ overestimated and a decreasing trend of κ will cause the measured κ underestimated.

3.2 Multi-charge correction for mixing state

Except for the size-resolved mean hygroscopicity, the key information that can be obtained from the HTDMA also includes
145 the mixing state and the detailed shape of GF-PDF or κ -PDF. The correction of GF-PDF or κ -PDF involves the inversion of two-dimensional vectors, which is too complicated for this study. But the mixing state can be simply represented by the particle number fraction in different GF ranges. Here, we can use the number fraction of Less-Hygroscopic particles as an example.

The correction for mixing state is similar in general to the correction for mean hygroscopicity, but differ in some minor
150 aspects. When the scan diameter in DMA is set as D_i , the observed number fraction of less-hygroscopic particles by HTDMA can be expressed as:



$$A_i = \frac{1}{N(i)} \int_0^\infty G^*(i, x) A^*(x) n(x) dx \quad (11)$$

where the A_i is the measured number fraction of LH group particles at the DMA selected diameter D_i ; the $A^*(x)$ represents the true number fraction at scale parameter x .

$$155 \quad G^*(i, x) = \sum_{v=1}^\infty F(x, v) \Omega(x, v, i) C(i, x) \quad (12)$$

$$N(i) = \int_0^\infty G(i, x) n(x) dx \quad (13)$$

where the $C(i, x)$ represents the correction factor caused by the weakening effect. This factor varies with different GF-probability distribution function (GF-PDF) and cannot be simplified into a constant. If we assume that the weakening effect on the LH number ratio can be neglected, then this parameter is 1 and the question can be simplified into:

$$160 \quad A_i = \int_0^\infty H(i, x) A^*(x) \quad (14)$$

or

$$\mathbf{A} = \mathbf{H} \mathbf{A}^* \quad (15)$$

where $H(i, x)$ is:

$$H(i, x) = \frac{1}{N(i)} n(x) G(i, x) dx \quad (16)$$

165 The $H(i, x)$ or the \mathbf{H} matrix can also be calculated from given information. One hypothetical $A(x)$ distributions along with the corresponding multi-charge corrected $A(x)$ distributions are also shown in Fig.4.

4 Application in field measurements

During the winter of 2019, a comprehensive aerosol field measurement focusing on hygroscopicity properties over size range of 50-600 nm was conducted at a Beijing urban site. During the measurement, an HTDMA instrument was employed to measure hygroscopic growth factors of particles with dry diameter of 50, 100, 200, 300, 400, 500, and 600 nm at 85% RH. Particle number size distributions (PNSD) were also measured by a BMI scanning electrical mobility sizer (BMI SEMS, Model 2100) with a size range of 10-1000 nm. In the measurement, a PM10 impactor was used to remove particles with aerodynamic diameter larger than 10 μm .

175 To evaluate the effects of multiply charged particles on the size-resolved hygroscopicity, we choose two weeks' measurement data to do the multi charge correction. The particle number size distribution and measured size-resolved hygroscopicity κ are shown in Fig. 6. For better comparison, we also present the size-resolved difference between measured and corrected hygroscopicity data. What's to be noted is that, since the upper limit of hygroscopicity measurement is 600 nm, the hygroscopicity in the higher size range is assumed to decrease linearly to 0 at 1 μm . Here we presume the
 180 hygroscopicity for coarse mode particles is 0. For particles larger than 1 μm , the number concentration is also assumed to decrease linearly to 0 at 1.2 μm in the multi-charge correction.



Generally, for particles less than 200 nm, particle's hygroscopicity will be overestimated. For particles larger than 200 nm, particle's hygroscopicity will be underestimated. From Fig. 6(b), we can see that in the urban environment, the hygroscopicity often peaks at the size range of 200-400 nm. The relatively high hygroscopicity in this size range will be
185 mixed into the lower size in the HTDMA measurement, leading to a false increase of measured κ . Similarly, most of the ambient particles have a relatively lower hygroscopicity in the upper size. When they carry multiple charges and sneak into to the lower accumulation size set by the DMA, the hygroscopicity in the target size region will be lowered.

The overall difference between corrected and measured size-resolved κ mostly lie within 0.05. For the electrical mobility size that affected most by multi-charge particles, e.g. 100 nm, the doubly or triply charged particles correspond to 151 nm
190 and 196 nm. These three sizes normally share similar hygroscopicity, which leads to a small effect on the measured κ . However, when there exists a large variation of hygroscopicity in these three sizes, the multi-charge correction in this size will be necessary. For particles larger than 300 nm, the multi-charge effect is mostly contributed by particles larger than 500 nm. Few field observations on hygroscopicity have covered this size range, which brought large uncertainty to the multi-charge correction. From our measurement, the variation of hygroscopicity in this size range is relatively large, depending on
195 different pollution conditions. On average, the hygroscopicity of particles above 500 nm is lower than other accumulation sizes. Because of the assumption of few particles above 1 μm , the multi-charge effect on the size above 500 nm is fairly small. In practice, this can be achieved by installing an impactor before the inlet of the first DMA.

5 Conclusion

The HTDMA instrument has been extensively used in numerous field measurements to obtain the hygroscopic properties of
200 submicron particles. Aerosol particles sampled by the DMA are quasi-monodisperse with different charges and different diameters. Thus, size-resolved hygroscopicity measured by DMA will be influenced by the contribution of multiply charged aerosols. In the hygroscopicity measurement by HTDMA, this effect has seldom been discussed in previous field measurements.

In this study, we firstly demonstrate that the multi-charge not only influence the hygroscopicity measurement through the
205 number contribution, but also through the weakening effect. On one hand, the number fraction of multiply charged particles is quite considerable, especially under polluted conditions. Results show that there can be 30% to 40% of selected particles are mistaken from large multiply charged particles in the polluted period. On the other hand, the growth factor or hygroscopicity measured by the HTDMA can be smaller than the true value for multiply charged particles, which is also called the multi-charge weakening effect. This effect can be quantified as a weakening factor using the electrical mobility
210 theory. The weakening factor reaches its peak around the size of 200 nm and increases with the number of charges the particle carries.



We propose an algorithm to do the multi-charge correction for the size-resolved hygroscopicity κ and mixing state. The algorithm is based on the principle of SMPS multi-charge correction and the knowledge of aerosol PNSD is required. The key in this algorithm is to obtain the forward function and to solve the inverse problem.

215 The proposed multi-charge correction is applied in a field measurement to evaluate the multi-charge effects. The relatively high hygroscopicity in accumulation size range will lead to overestimation of the particle's hygroscopicity smaller than 200 nm. The low hygroscopicity in coarse mode particles will lead to the underestimation of accumulation particles. The difference between measured and corrected κ can reach as large as 0.05.

The measured hygroscopicity between 200 nm and 400 nm is influenced by multiply charged particles larger than 400 nm, 220 indicating that the hygroscopic measurement above 400 nm is necessary if correct hygroscopic properties want to be obtained for accumulation mode particles. For particles larger than 400 nm, the multi-charge effect can be removed by installing an impactor with cutting size around 1 μm or even lower. In the future hygroscopicity measurements, our studies highlight that special attention should be paid to the multi-charge effects, and multi-charge correction should be done if accurate size-resolved hygroscopicity needs to be obtained.

225

Competing interests. The authors declare that they have no conflict of interest.

Data availability. The data used in this study is available when requesting the authors.

Author contributions. Chuanyang Shen, Gang Zhao and Chunsheng Zhao discussed the results; Chuanyang Shen wrote the 230 manuscript.

Acknowledgements. This work is supported by the National Natural Science Foundation of China (41590872).

235



References

- ALBRECHT, B. A. (1989). Aerosols, Cloud Microphysics, and Fractional Cloudiness. *Science*, 245(4923), 1227-1230. doi:10.1126/science.245.4923.1227
- 240 Chang, D., Song, Y., & Liu, B. (2009). Visibility trends in six megacities in China 1973–2007. *Atmospheric Research*, 94(2), 161-167. doi:10.1016/j.atmosres.2009.05.006
- CHARLSON, R. J., SCHWARTZ, S. E., HALES, J. M., CESS, R. D., COAKLEY, J. A., HANSEN, J. E., & HOFMANN, D. J. (1992). Climate Forcing by Anthropogenic Aerosols. *Science*, 255(5043), 423-430. doi:10.1126/science.255.5043.423
- 245 Cubison, M. J., Coe, H., & Gysel, M. (2005). A modified hygroscopic tandem DMA and a data retrieval method based on optimal estimation. *Journal of Aerosol Science*, 36(7), 846-865. doi:10.1016/j.jaerosci.2004.11.009
- Deng, Z. Z., Zhao, C. S., Ma, N., Liu, P. F., Ran, L., Xu, W. Y., . . . Wiedensohler, A. (2011). Size-resolved and bulk activation properties of aerosols in the North China Plain. *Atmospheric Chemistry and Physics*, 11(8), 3835-3846. doi:10.5194/acp-11-3835-2011
- 250 Duplissy, J., Gysel, M., Alfarra, M. R., Dommen, J., Metzger, A., Prevot, A. S. H., . . . Baltensperger, U. (2008). Cloud forming potential of secondary organic aerosol under near atmospheric conditions. *Geophysical Research Letters*, 35(3). doi:10.1029/2007gl031075
- Guo, Jianping, Su, Tianning, Li, Zhanqing, . . . Liu. (2017). Declining frequency of summertime local-scale precipitation over eastern China from 1970 to 2010 and its potential link to aerosols. *Geophysical Research Letters*.
- 255 Gysel, M., McFiggans, G. B., & Coe, H. (2009). Inversion of tandem differential mobility analyser (TDMA) measurements. *Journal of Aerosol Science*, 40(2), 134-151. doi:10.1016/j.jaerosci.2008.07.013
- Haywood, J., & Boucher, O. (2000). Estimates of the direct and indirect radiative forcing due to tropospheric aerosols: A review. *Reviews of Geophysics*, 38(4), 513-543. doi:10.1029/1999rg000078
- Ibald-Mulli, A., Wichmann, H. E., Kreyling, W., & Peters, A. (2002). Epidemiological Evidence on Health Effects of Ultrafine Particles. *Journal of Aerosol Medicine*, 15(2), 189-201. doi:10.1089/089426802320282310
- 260 Kreidenweis, S. M., & Asa-Awuku, A. (2014). Aerosol Hygroscopicity: Particle Water Content and Its Role in Atmospheric Processes. 331-361. doi:10.1016/b978-0-08-095975-7.00418-6
- Lohmann, U., & Feichter, J. (2005). Global indirect aerosol effects: a review. *Atmos. Chem. Phys.*, 5(3), 715-737. doi:10.5194/acp-5-715-2005
- 265 Penner, J. E., Hegg, D., & Leaitch, R. (2001). Unraveling the role of aerosols in climate change. *Environmental Science & Technology*, 35(15), 332A-340A. doi:10.1021/es0124414
- Petters, M., & Kreidenweis, S. (2007). A single parameter representation of hygroscopic growth and cloud condensation nucleus activity. *Atmospheric Chemistry and Physics*, 7(8), 1961-1971.
- 270 Stolzenburg, M. R., & McMurry, P. H. (2008). Equations Governing Single and Tandem DMA Configurations and a New Lognormal Approximation to the Transfer Function. *Aerosol Science and Technology*, 42(6), 421-432. doi:10.1080/02786820802157823
- Su, T., Li, J., Li, C., Kai-Hon Lau, A., Yang, D., & Shen, C. (2017). An intercomparison of AOD-converted PM_{2.5} concentrations using different approaches for estimating aerosol vertical distribution. *Atmospheric Environment*, 531-542.
- 275 Swietlicki, E., Hansson, H. C., Hämeri, K., Svenningsson, B., Massling, A., McFiggans, G., . . . Kulmala, M. (2017). Hygroscopic properties of submicrometer atmospheric aerosol particles measured with H-TDMA instruments in various environments—a review. *Tellus B: Chemical and Physical Meteorology*, 60(3), 432-469. doi:10.1111/j.1600-0889.2008.00350.x
- Twomey, S. (1974). Pollution and the planetary albedo. *Atmospheric Environment (1967)*, 8(12), 1251-1256. doi:[http://dx.doi.org/10.1016/0004-6981\(74\)90004-3](http://dx.doi.org/10.1016/0004-6981(74)90004-3)
- 280 Voutilainen, A., Stratmann, F., & Kaipio, J. P. (2000). A NON-HOMOGENEOUS REGULARIZATION METHOD FOR THE ESTIMATION OF NARROW AEROSOL SIZE DISTRIBUTIONS. *Journal of Aerosol Science*, 31(12), 1433-1445. doi:[https://doi.org/10.1016/S0021-8502\(00\)00044-6](https://doi.org/10.1016/S0021-8502(00)00044-6)
- Wiedensohler, A., Lütke-meier, E., Feldpausch, M., & Helsper, C. (1986). Investigation of the bipolar charge distribution at various gas conditions. *Journal of Aerosol ence*, 17(3), 413-416.



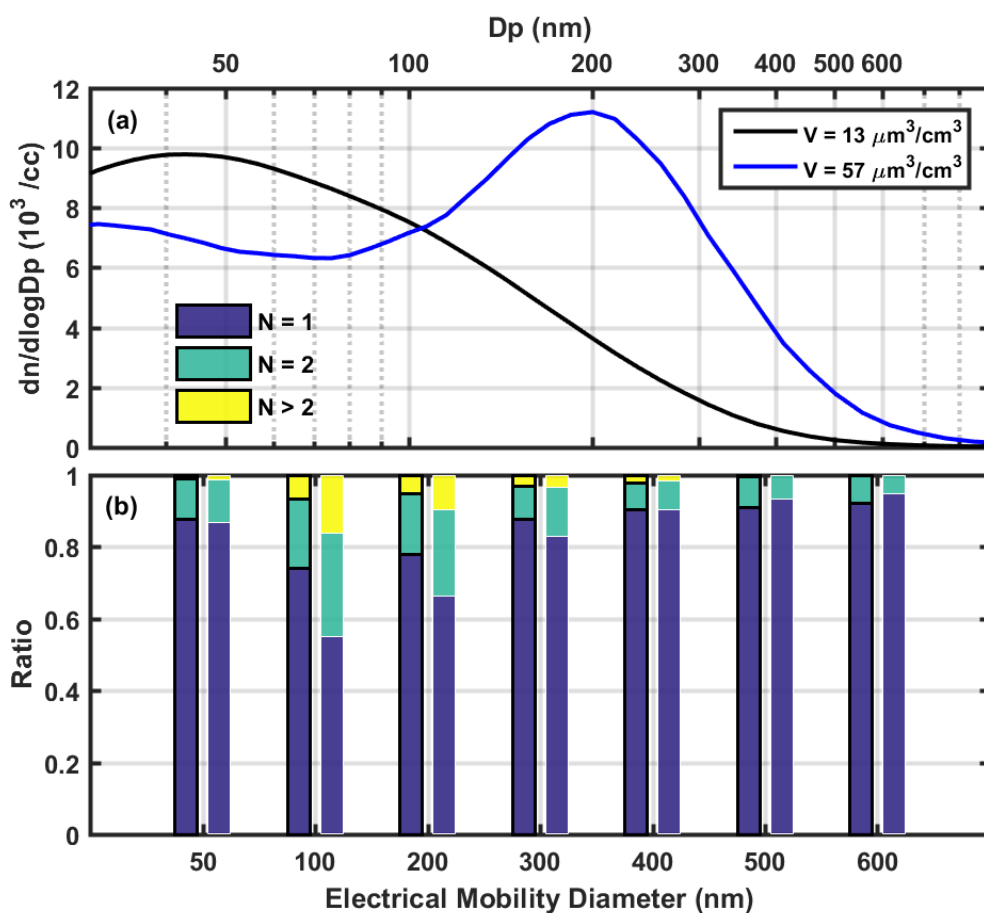
- 285 Zhao, G., Tao, J., Kuang, Y., Shen, C., Yu, Y., & Zhao, C. (2019). Role of black carbon mass size distribution in the direct aerosol radiative forcing. *Atmospheric Chemistry and Physics*, 19(20), 13175-13188. doi:10.5194/acp-19-13175-2019

290

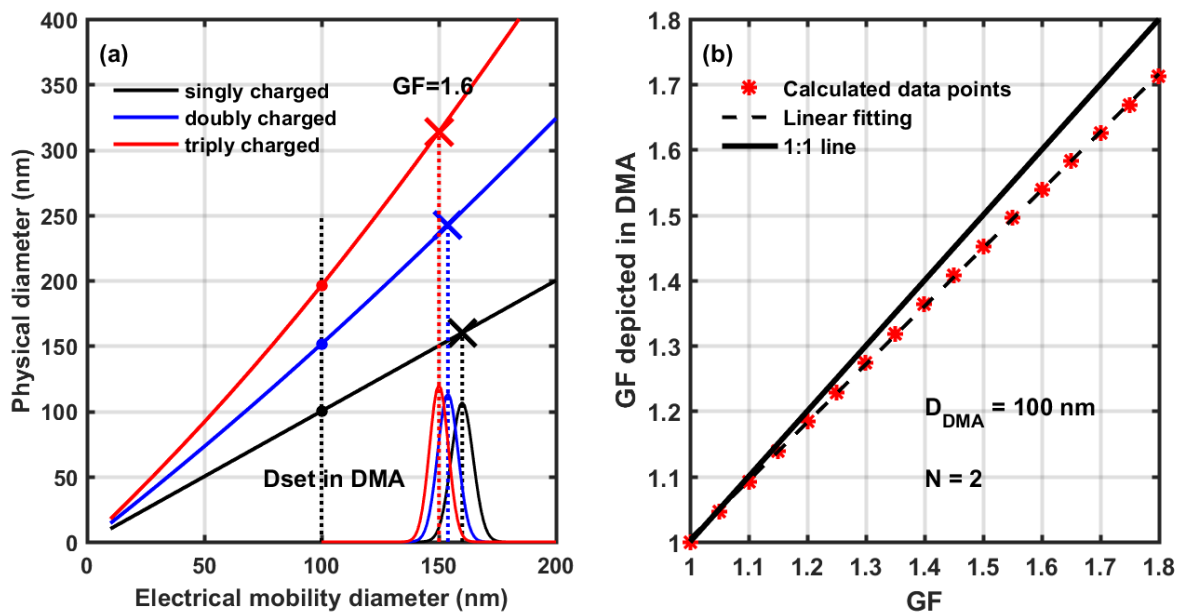
Table 1 The weakening factor of aerosol particle's hygroscopicity under 85% RH over different electrical mobility diameters.

Dp (nm) N	50	100	200	300	400	500	600
1	1	1	1	1	1	1	1
2	0.98	0.90	0.85	0.86	0.87	0.89	0.90
3	0.95	0.82	0.77	0.80	0.83	0.85	0.86
4	0.92	0.77	0.73	0.77	0.80	0.82	0.84
5	0.89	0.74	0.71	0.75	0.78	0.81	0.83

295



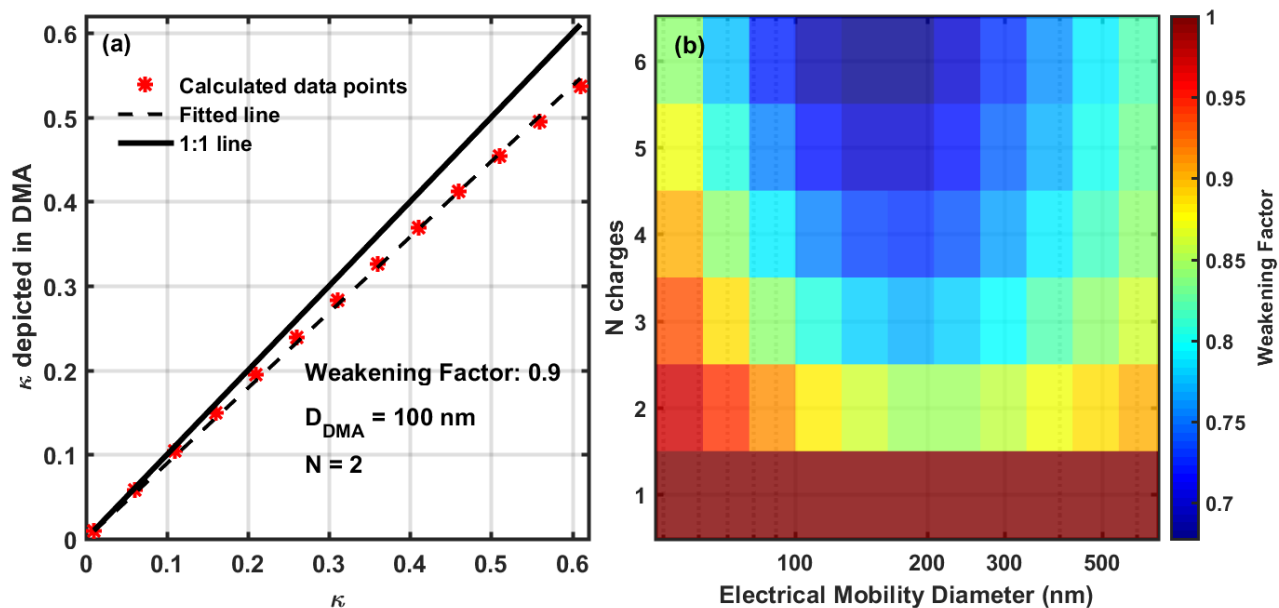
300 Figure 1. (a) Two cases of particle number size distribution during the field measurement. The black line represents the relatively clean period and the blue line represents the heavily polluted period. (b) The number ratio of particles carrying different charges. The left bar with black edge color corresponds to the PNSD in black line; the right bar without edge color corresponds to the PNSD in blue line.



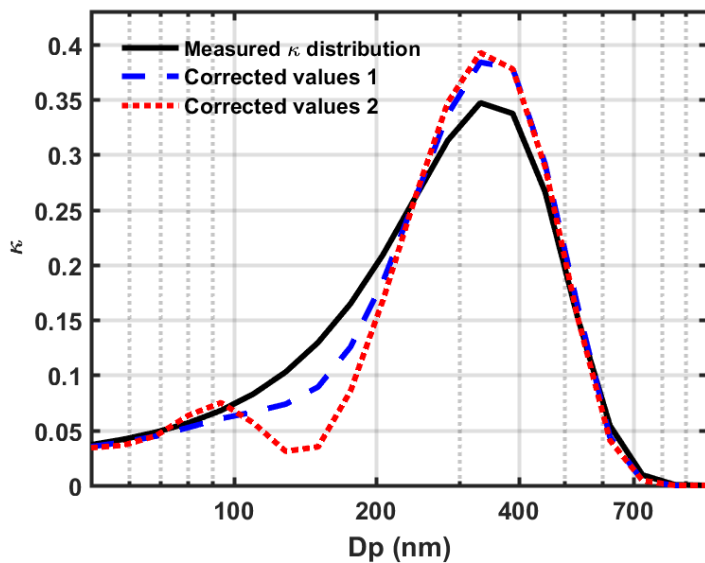
305

Figure 2. (a) Effects of particle carrying multiple charges; black, blue and red lines represent singly, doubly and triply charges particles, respectively. The circle points are particles selected by DMA when the electrical mobility diameter is set as 100 nm. When the true growth factor is 1.6, these particles will grow to the corresponding crossed points. The mode of the MDF of multiply charged particles peaks at a smaller GF than the true value. (b) The weakening effect of different growth factors for doubly charged particles with an electrical diameter of 100 nm.

310



315 Figure 3. (a) The weakening effect of different hygroscopicity (under 85% RH) for doubly charged particles with an electrical mobility diameter of 100 nm. The fitted slope or weakening factor is 0.8953. (b) A summary of weakening factors for different electrical mobility diameters carrying different number of charges at 85% RH.



320

Figure 4. Multi-charge correction for a hypothetical κ distribution. The black line is the measured size-resolved κ and the dashed lines are the multi-charge corrected κ distributions based on different number size distributions. The used PNSD can be referred to in Fig. 1.

325

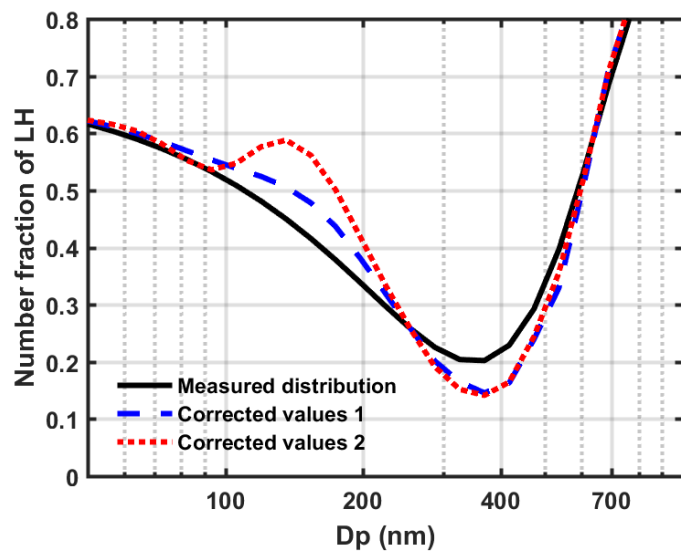
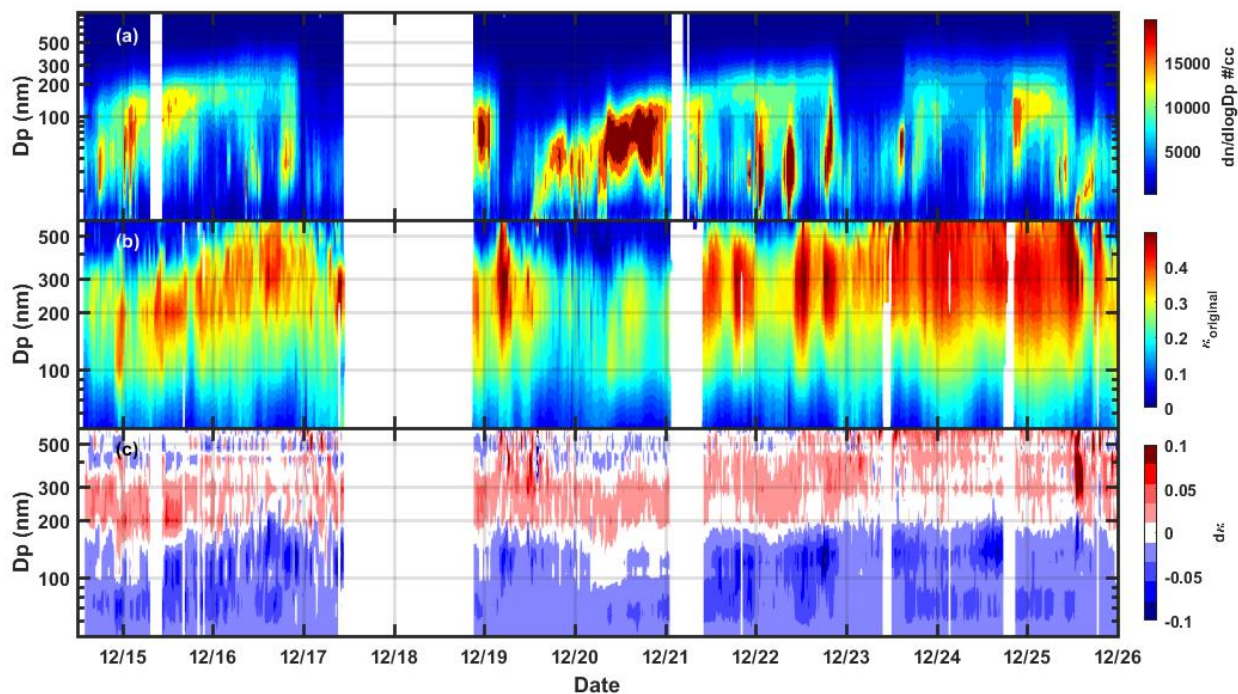


Figure 5. Multi-charge correction for one hypothetical mixing state distribution. The black lines are the measured size-resolved number fraction of LH and the dashed lines are the multi-charge corrected values based on different number size distributions.



330

Figure 6. The field measurement of the PNSD and size-resolved hygroscopicity in Beijing winter. (a) The filled color gives the particle number concentration over different diameter (D_p). (b) The filled color represent the size-resolved hygroscopicity parameter κ . (c) The difference between measured and multi-charge corrected κ . $d_\kappa = \kappa_{corrected} - \kappa_{measured}$.